U N I V E R S I T Y   O F   R E A D I N G

ROE'S SCHEME, EULER EQUATIONS, CARTESIAN GRIDS, NON-CARTESIAN GEOMETRIES, RIGID WALLS AND THERE'S MORE

A. Priestley

Numerical Analysis Report 9/88

University of Reading
Department of Mathematics
P.O. Box 220
Reading RG6 2AX

M A T H E M A T I C S   D E P A R T M E N T

ROE'S SCHEME, EULER EQUATIONS, CARTESIAN GRIDS, NON-CARTESIAN GEOMETRIES, RIGID WALLS AND THERE'S MORE

A. Priestley

Numerical Analysis Report 9/88

University of Reading
Department of Mathematics
P.O. Box 220
Reading RG6 2AX

The work reported here forms part of the research programme of the Reading/Oxford Institute for Computational Fluid Dynamics and has been supported by the S.E.R.C. Grant No. GR/E72256.

Introduction

This report follows on from an earlier report by Priestley (1987) and pursues the ideas expressed there. That is, we are concerned with solving the Euler equations using Roe's scheme on Cartesian grids but to predict flows around non-cartesian bodies. Whilst body-fitted grids are aesthetically very pleasing, the practicalities of three-dimensional aeronautical configurations has led some researchers to rediscover their roots and return to the use of Cartesian meshes rather than slavishly following the trend towards adaptive and body-fitted meshes.

Some notable, although by no means exclusive, work with cartesian meshes has been done by Clarke et al (1986), Leveque (1988) and Moretti and Dadone (1988).

In this report the work is in two sections. Firstly there is a direct application of the previous report to the flow past a HERMES type forebody. This problem forced the author to revise his opinions on generating regular Cartesian meshes.

In the second section we turn our attention to three dimensions. One major reason for using Cartesian meshes is the ease of extension to 3-D, but the problem, as in 2-D, is the imposition of rigid wall boundary conditions. In this section we will show how this can be done and present results for a test problem.

1. DOUBLE ELLIPSE PROBLEM

This is a GAMM workshop problem designed to test research codes around an analytic, but realistically shaped body. The double ellipse problem is a 2-D version of the double ellipsoid problem and is defined below.

Lower Surface:

$$y = -0.015 \qquad 0 \leq x \leq 0.016$$

$$y = -0.015\sqrt{1-\left[\frac{x}{0.06}\right]^2} \qquad -0.06 \leq x \leq 0$$

Upper Surface:

$$y = 0.025 \qquad 0 \leq x \leq 0.016$$

$$y = 0.025\sqrt{1-\left[\frac{x}{0.035}\right]^2} \qquad x^* \leq x \leq 0$$

$$y = 0.015\sqrt{1-\left[\frac{x}{0.06}\right]^2} \qquad -0.06 \leq x \leq x^*$$

where $x^* = -0.029890588$.

Figure 1 shows the body defined by these formulae. The two flow regimes that will be considered both have freestream Mach numbers of 8.15, the first having an angle of attack of 0^o and the second of 30^o.

1.1 The Grid

We need to produce a Cartesian mesh fine enough to resolve the body and all interesting features of the flow caused by it, and coarse enough to reach the farfield moderately quickly.

In Priestley (1987) two attempts were made to address this question. Firstly, and most simply, a tensor product grid was used. This certainly allows a fine mesh to be constructed around the body but no matter how quickly the x-mesh or y-mesh is then stretched there will always be a preponderance of cells immediately above, below, left and right of the body. This results in much unnecessary work. The way forward, according to this report, was to take a very coarse mesh and then to refine this around the body and any interesting flow features. Whilst this procedure is very efficient in terms of the number of cells needed, virtually all the advantages of having a Cartesian mesh are lost due to the irregularity of the resulting grid.

Inspired by a talk of Moretti (1988) (although no doubt the ideas go back further than that), for the double ellipse problem it was decided to use totally uniform Cartesian grids. This reduces upwind schemes to their simplest forms and reduces the amount of housekeeping needed virtually to zero. It is also easy to see how a fine mesh can be constructed to cover the body and sharpest flow features. Constructing a mesh coarse enough to reach the farfield quickly is also easily envisaged. Reconciling the two is also surprisingly straightforward. That is we simply use both meshes. Indeed, for the double ellipse problem, four meshes were used. No claims are made that the best nesting of meshes has been used - the inner mesh could do to be finer - the coarsening of the meshes could do to be quicker. However, we hope that the respectable solutions obtained will convince the reader of the wisdom of this approach and that any disquiet envisaged with the passing of data from one grid to another is ill-founded.

1.2 Passing of Data

It is important that the passing of information between the grids does not present any problems, as it is almost certain that we will not be able to afford to capture, completely, the features we are interested in on the finest mesh. The pictures presented later show this to be the case but the solution does not seem to suffer. This is accomplished by ensuring that the grids are all overlapping in the following manner (see Figure 2).

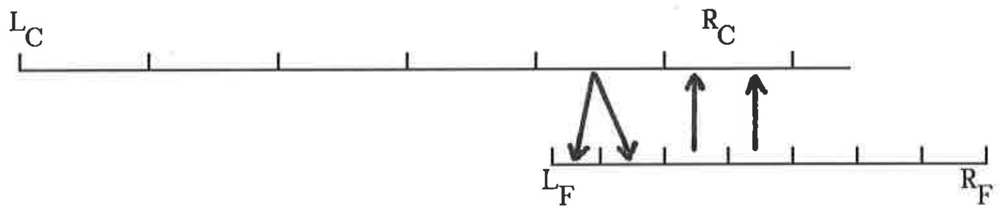

Figure 2

This one-dimensional example shows how the information is transferred. After performing an iteration on the fine-mesh (cells $L_F \rightarrow R_F$) the values in cells L_{F+2} and L_{F+3} are used to update the value on the right-hand boundary cell of the coarse mesh, R_C. After an iteration has been performed on the coarser mesh, the new value in R_{C-1} is then used to update the values at L_{F+1} and L_F on the fine mesh.

An exactly analogous procedure can be used in two dimensions. With multiple grids this means that the CFL number will change drastically from the finest mesh to the coarsest. Although, for the steady state problems we are attempting here, local time-stepping would be permissible, our real interest is in evolutionary problems. Moreover, due to the extreme regularity of the grids it is possible to calculate a time-accurate solution without being hindered by CFL numbers of different orders of magnitude.

With a twofold increase, as in figure 2, between grids and using 4 grids in total we choose a DT for the finest grid (grid 1). The time-step on the second mesh is 2DT, on the third mesh 4DT and on the fourth 8DT.

We then perform two time-steps on the finest mesh before doing a time-step on the second mesh. This process is repeated before doing a time-step on the third mesh. Eventually we will do a time-step on the coarsest mesh having done 8 on the finest, 4 on the second and 2 on the third. We can modify this procedure, if a time-accurate solution is not required, by changing the number of time-steps we do before moving up to the coarser grid.

An advantage of the overlapping grids that we have yet to take advantage of is the possibility of performing a Richardson extrapolation to improve the accuracy. This would perhaps not be an advisable procedure in the vicinity of the discontinuities but in the smoother regions of the flow it may be possible to enhance the results somewhat at no extra cost.

1.3 Results

Figures 3-6 are for the zero incidence case and show density (ρ/ρ_∞), pressure coefficient ($(p-p_\infty) / \frac{1}{2}\rho_\infty u_\infty^2$), mach number and a global density plot. Apologies are made for the uninformative plot of C_p. This was due to a poor choice of contours. Figures 7 - 10 show the same sequence for the thirty degree case. Figure 11 shows a typical arrangement of the grids.

These results all look very plausible. However, it has been pointed out to the author that the canopy shock in the zero incidence case could do to be closer to the canopy (see Gustafsson (1988), for example). There are two reasons why we may have got this wrong. Firstly the grid could do to be finer around the body - it is hoped to remedy this situation in the near future. Secondly there is the business of calculating the information required by the boundary routine. The procedure described by this author (1987) requires the code to look for a basic stencil and rotations and reflections thereof. In 3-D this approach seemed oppressively complex and unmanageable. After a little thought a much simpler procedure was arrived at, to be described in the next section. It is hoped that this 3-D routine can now be altered to provide a more robust 2-D version and hence eliminate this question mark. However, even with these doubts the results are quite believable and in particular there are no problems at grid boundaries.

2. RIGID WALLS IN THREE-DIMENSIONS

Following the success of the two-dimensional tests of using Cartesian grids (even though the body may be distinctly non-cartesian), the next stage was to extend the idea to three dimensions where the advantages of uniform meshes over body-fitted or adaptive meshes become even more significant. How then to pursue this approach in 3-D?

In two dimensions the (curved) boundary was replaced by a series of straight lines. In three dimensions the obvious procedure is to replace the (curved) surface by a set of flat plates.

Consider the point (i,j,k) at the centre of a block of 27 points $\{ (i\pm1, j\pm1, k\pm1) \}$, see Figure 12.

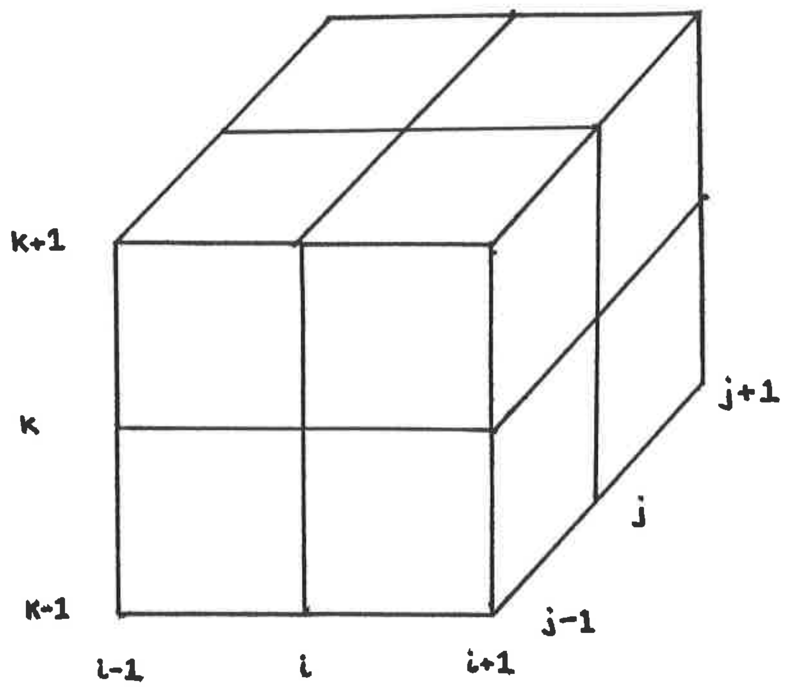

Figure 12

We now assume that we have certain information available to us concerning the body surface:-

1. A function INSIDE (x,y,z) that given a point in space returns a value of 1 or 0 according to whether the point is within the body or not.

2. A function $z(x,y)$ that given a point (x,y) returns the value of z that lies on the surface.

3. Functions $\frac{\partial z(x,y)}{\partial x}$ and $\frac{\partial z(x,y)}{\partial y}$ that return derivatives of the above function.

4. Similarly defined functions $x(y,z)$, $y(x,z)$, $\frac{\partial x}{\partial y}$, $\frac{\partial x}{\partial x}$, $\frac{\partial y}{\partial x}$, $\frac{\partial y}{\partial z}$.

The procedure is now as follows.

(a) If the point, (i,j,k), does not lie inside the body, then get the next point, else go to (b).

(b) We now need to decide if the point is on the boundary. This is done by looking at the three pairs of points $\{x_{i-1}, x_{i+1}\}$, $\{y_{j-1}, y_{j+1}\}$ and $\{z_{k-1}, z_{k+1}\}$. If there exists a pair for which one point is inside and the other outside, then the point (i,j,k) is a boundary point and we proceed to (c). If, for all 3 pairs, both points are either inside or outside, then the point is not on the boundary.

c. Let us assume that it was the $\{z_{k-1}, z_{k+1}\}$ pair that satisfied the criterion of (b). We now need to find the plane that locally approximates the surface.

The general equation of a plane is

$$ax + by + cz + d = 0.$$

Immediately we can put $c = -1$ (so that $z = z(x,y)$). The parameters a and b can be found straight away from the functions $\partial z/\partial x$ and $\partial z/\partial y$. We can also calculate the value of d although it is not actually needed.

d. We now have the plane and its normal, given by (a,b,c). Now we find a value, s, such that the point

$$(x_i, y_j, z_k) + s(a,b,c)$$

lies on the surface of the cube shown in Figure 12. This gives us the place from which we interpolate the values of (ρ, u, v, w, p) in order to apply the reflection conditions.

Call this point T, then

$$\rho_{i,j,k} = \rho_T$$
$$p_{i,j,k} = p_T.$$

For the velocities we need to reflect only the normal component leaving the tangential components unaltered. To resolve into normal and tangential components we need to solve

$$\begin{bmatrix} a & 1 & 1 \\ b & -a/b & b/a \\ c & 0 & -\left[\frac{a}{c} + \frac{b^2}{ac}\right] \end{bmatrix} \begin{bmatrix} \alpha \\ \beta \\ \gamma \end{bmatrix}_T = \begin{bmatrix} u \\ v \\ w \end{bmatrix}_T . \tag{2.1}$$

Calling the matrix in (2.1) Λ, the normal and tangential components at T are then given by

$$\underline{n}_T = \Lambda^{-1} \underline{u}_T .$$

To reflect the normal vector and obtain the normal and tangential components at (i,j,k) we multiply by a matrix D to get

$$\underline{n}_{ijk} = D \Lambda^{-1} \underline{u}_T$$

where $$D = \begin{bmatrix} -1 & 0 & 0 \\ 0 & 1 & 0 \\ 0 & 0 & 1 \end{bmatrix} .$$

To return to x,y,z velocities we now just need to multiply by Λ and so the final equation for the velocities at (i,j,k) is

$$\underline{u}_{ijk} = \Lambda D \Lambda^{-1} \underline{u}_T . \qquad (2.2)$$

Evaluating $\Lambda D \Lambda^{-1}$ explicitly leaves us with

$$\begin{bmatrix} u \\ v \\ w \end{bmatrix}_{ijk} = \begin{bmatrix} 1-\frac{2a^2}{R} & \frac{-2ab}{R} & \frac{-2ac}{R} \\ \frac{-2ab}{R} & 1-\frac{2b^2}{R} & \frac{-2bc}{R} \\ \frac{-2ac}{R} & \frac{-2bc}{R} & 1-\frac{2c^2}{R} \end{bmatrix} \begin{bmatrix} u \\ v \\ w \end{bmatrix}_T , \qquad (2.3)$$

where $R = a^2 + b^2 + c^2$.

2.1 The Results

A simple geometry has been chosen, namely a sphere with a Mach 8 free stream onflow. As I am sure most readers of this report in academic institutions in this country will appreciate, it was only possible to run this problem on a very coarse mesh (40,40,40) and for a very short time - 30 time-steps. Figure 13 shows a density plot at $k = 20$. Whilst this picture is far from being steady state and the mesh is far too crude for the results to be taken seriously, it is hoped the picture does demonstrate the possibilities of the approach.

3. CONCLUSIONS

It has been demonstrated that Cartesian grids can be used very successfully in conjunction with Roe's scheme to calculate flows past bodies of irregular shape, and that the procedure can be easily extended to three-dimensions, as has been shown in §3. More work needs to be done on the Hermes problem but this essentially appears to be tidying up and adjusting parameters rather than a major reappraisal. Roe's scheme on Cartesian grids is now looking a robust, generally applicable, competitive alternative for these types of problems.

4. ACKNOWLEDGEMENTS

Many thanks to Dr. Mike Baines and also to B. Calderon for the excellent typing. I acknowledge the support of the S.E.R.C..

5. REFERENCES

Clarke, D.K., Salas, M.D., and Hassan, H.A. (1986): "Euler Calculations for Multi Element Airfoils using Cartesian Grids", AIAA J. 24, 353-358.

Gustafsson, B. (1988): Results presented at the HERMES Hypersonics Workshop in Rome, May 1988.

Leveque, R.J. (1988): "Cartesian Grid Methods for Flow in Irregular Regions", To appear in the Proceedings of the Oxford Conference on Numerical Methods in Fluid Dynamics, March, 1988 (O.U.P.).

Moretti, G. and Dadone, A. (1988): "Airfoil Calculations in Cartesian Grids" To appear in the Proceedings of the II International Conference on Hyperbolic Problems, Aachen, March 1988 (Springer).

Priestley, A. (1987): "Roe's Scheme, Euler Equations, Cartesian Grids, non-Cartesian Geometries, Rigid Walls and All That", University of Reading, Numerical Analysis Report 14/87.

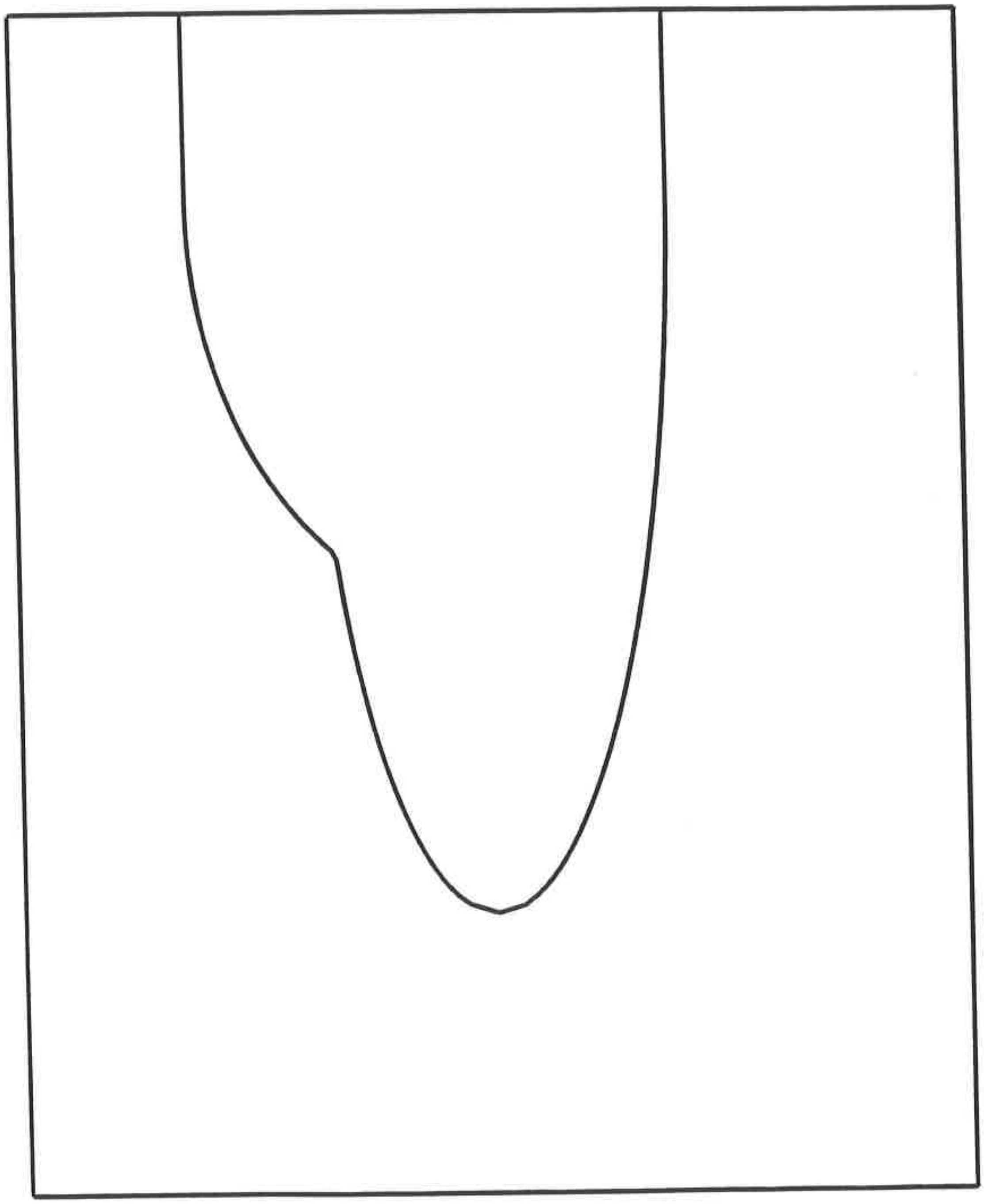

Figure 1: Forebody Geometry

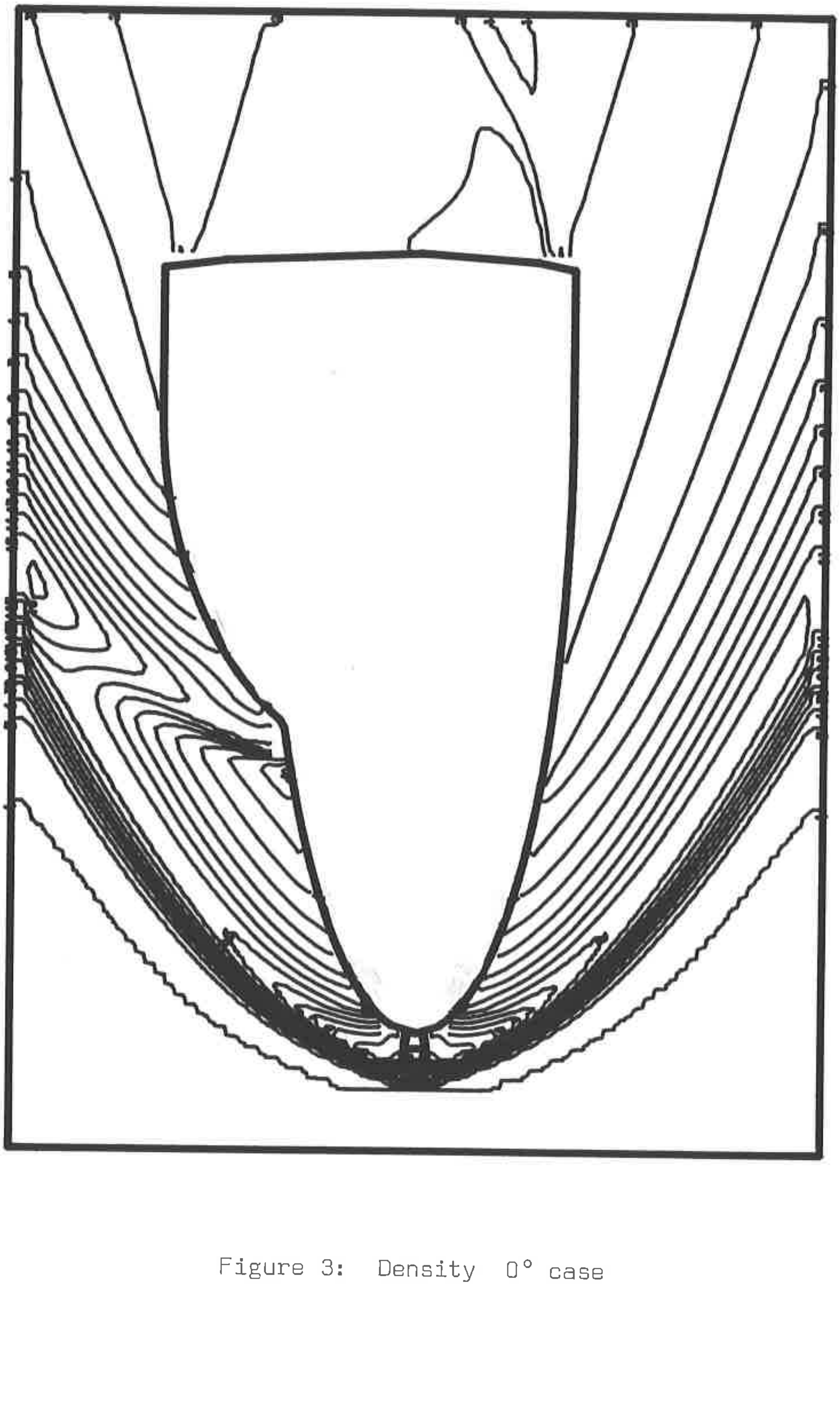

Figure 3: Density 0° case

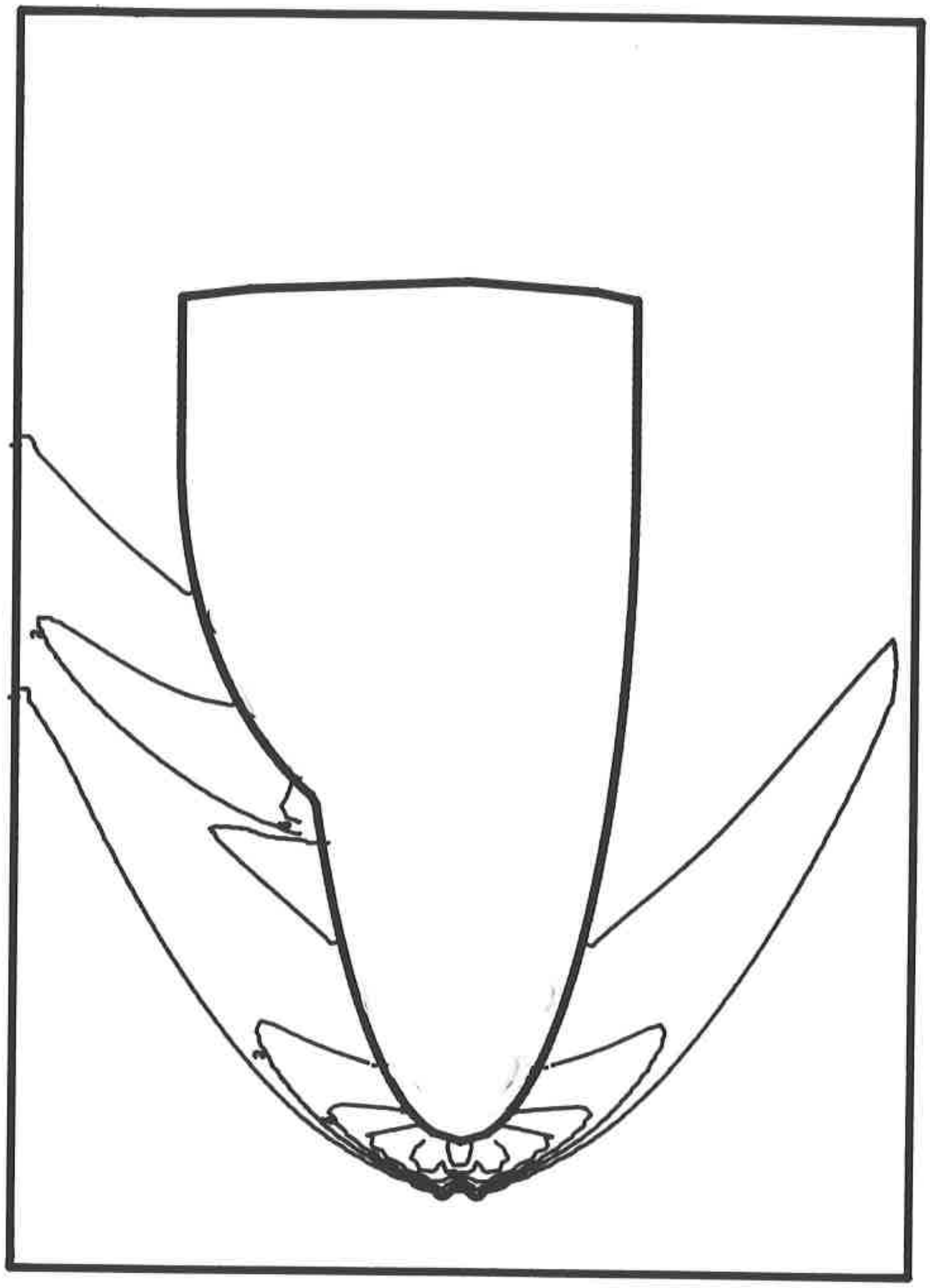

Figure 4: Pressure Coefficient 0° case

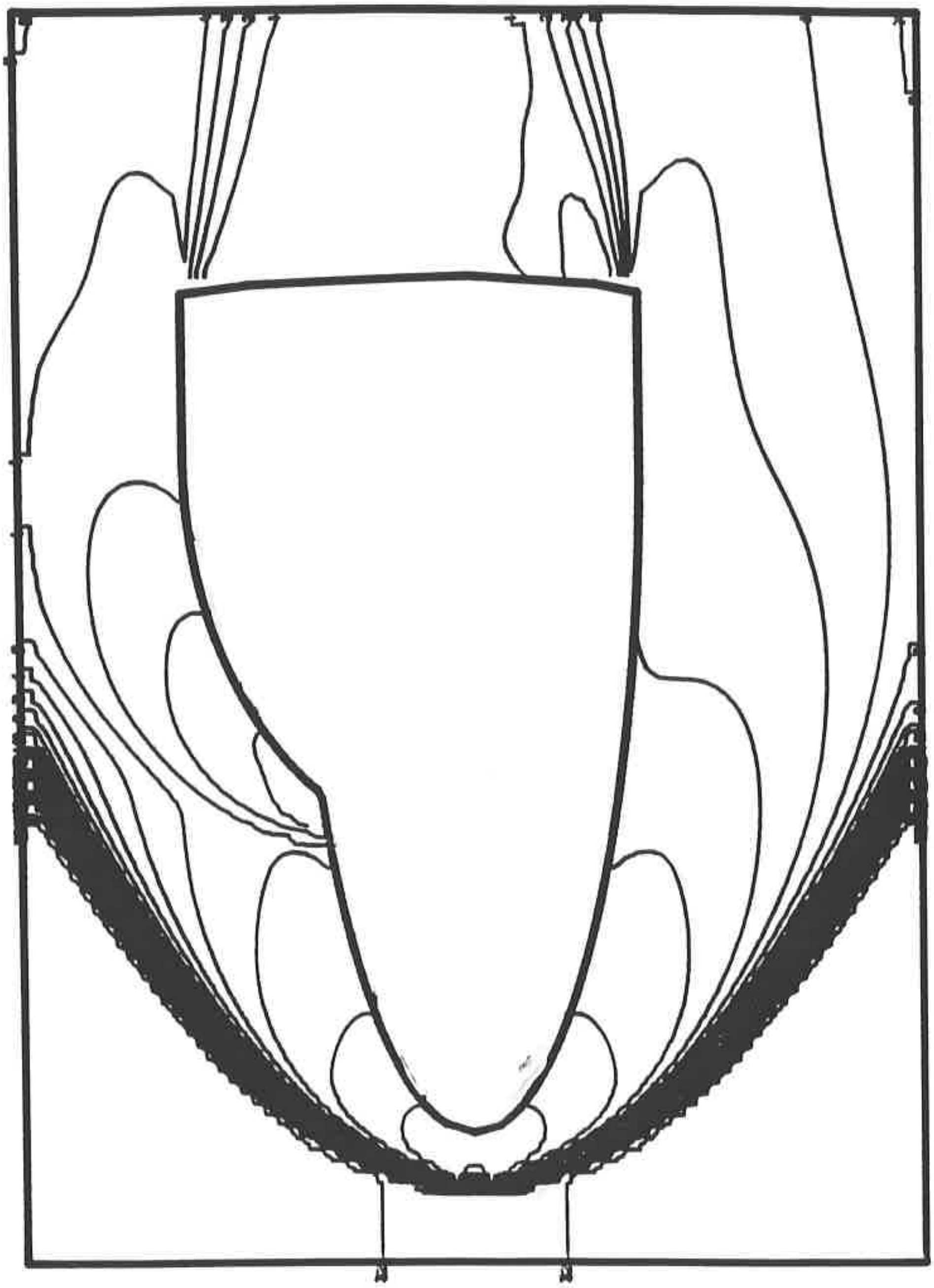

Figure 5: Mach number 0° case

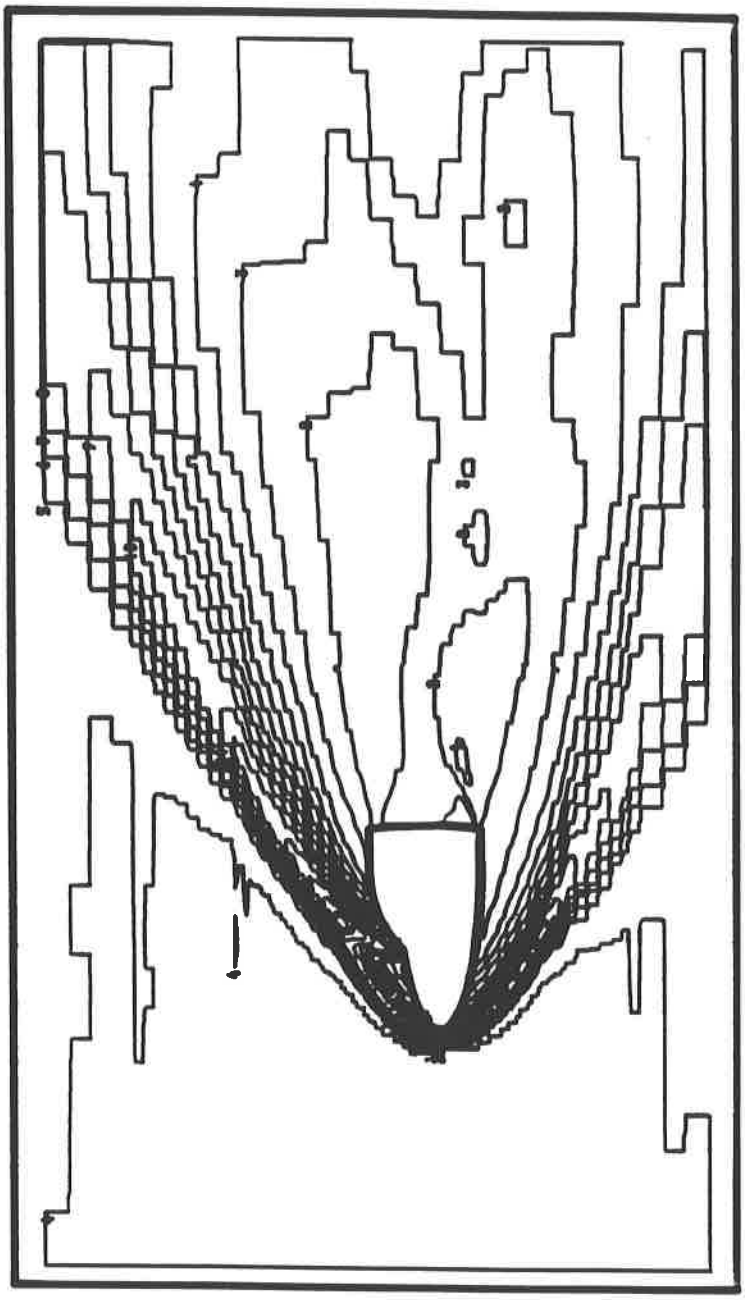

Figure 6: Density 0° case

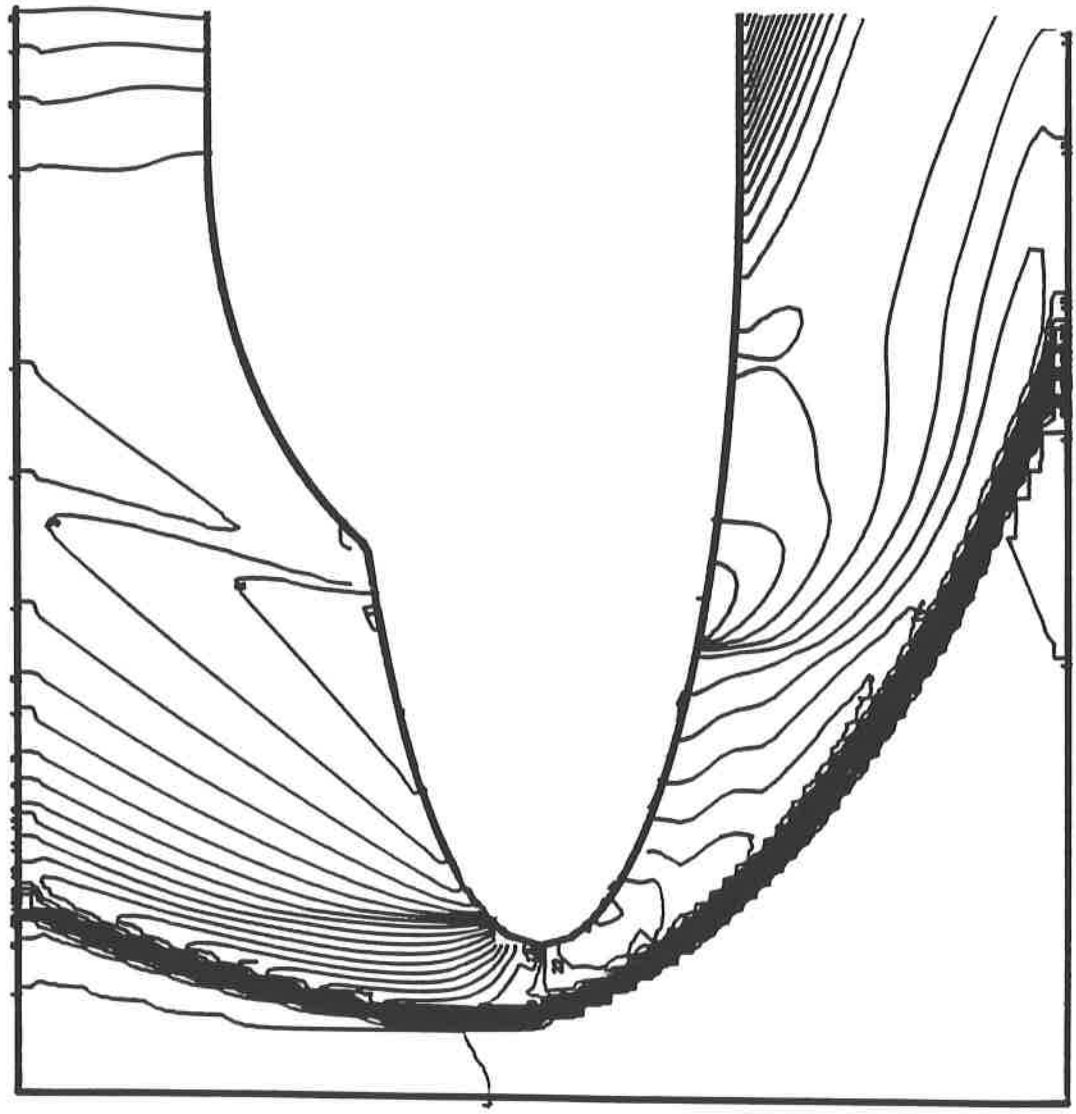

Figure 7: Density 30° case

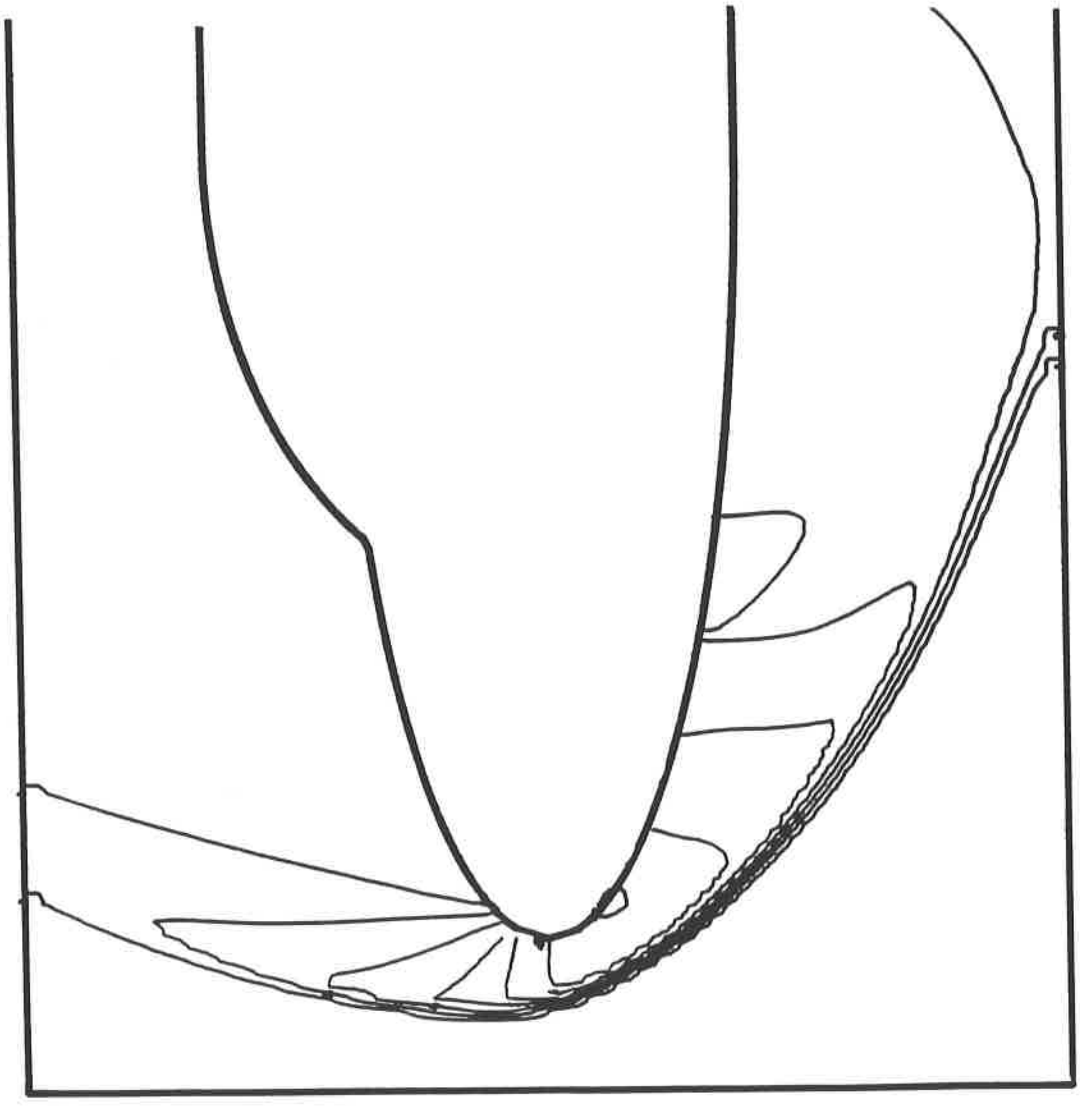

Figure 8: Pressure Coefficient 30° case

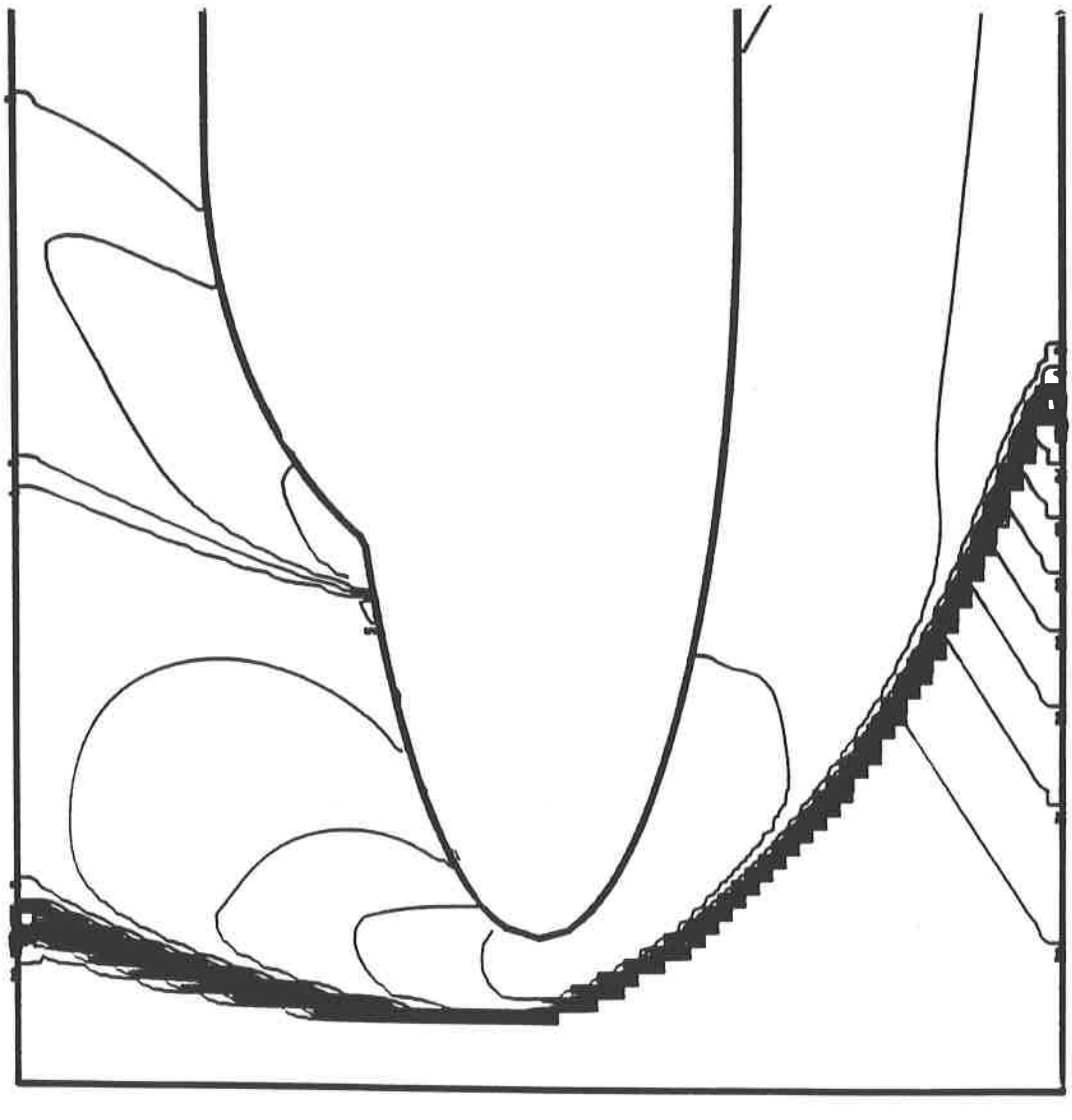

Figure 9: Mach number 30° case

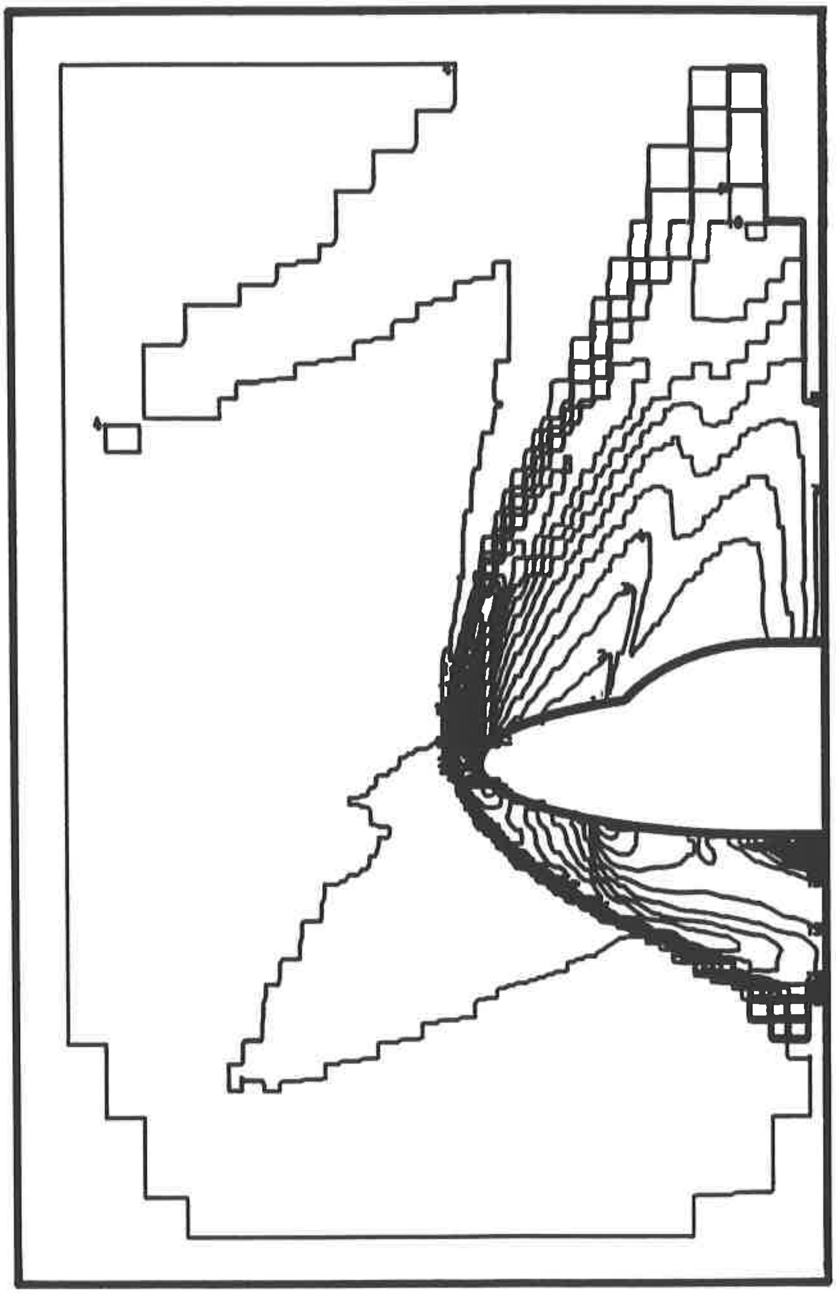

Figure 10: Density 30° case

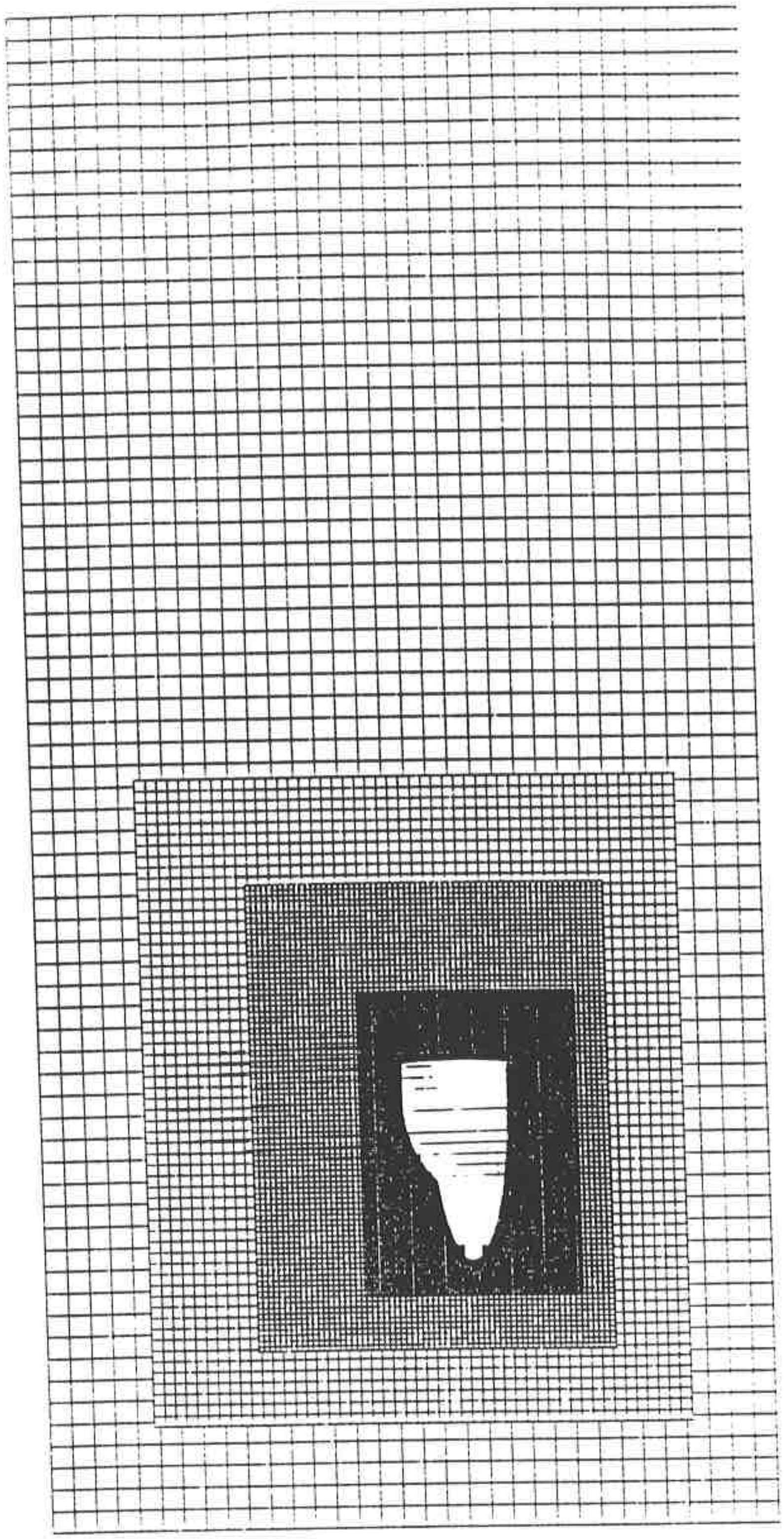

Figure 11

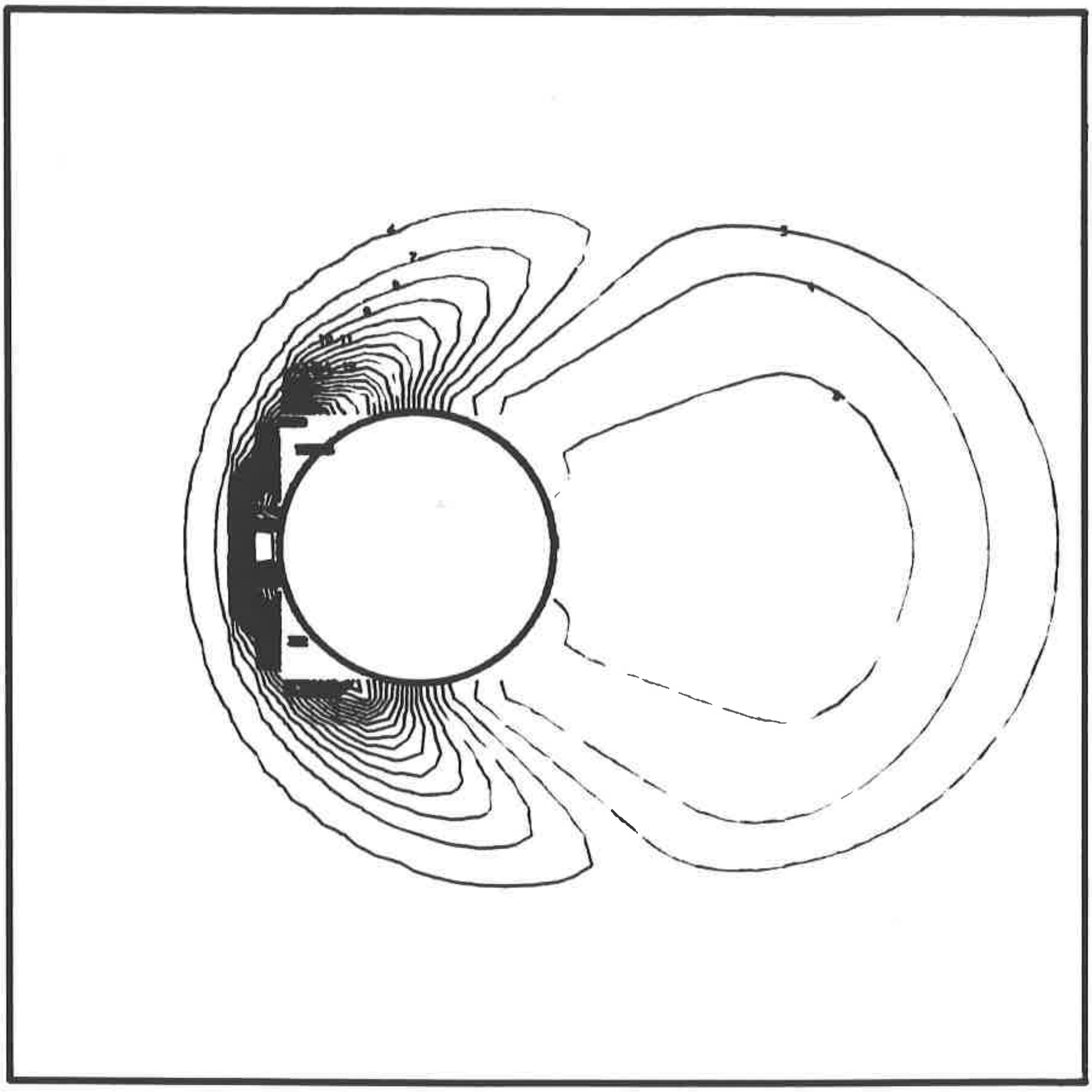

Figure 13: Density cross-section about sphere